



Development of activated carbon from *Eichhornia Crassipes* via chemical activation and its application to remove a synthetic dye

Sa'diah Salim¹, Tony Hadibarata^{2,*} , Elwina Elwina³ , Ratni Dewi³, Ibrahim A. Alaraidh⁴, Abdullah Ahmed Al-Ghamdi⁴, Abdulaziz A. Alsahli⁴

¹Department of Water and Environmental Engineering, Universiti Teknologi Malaysia, Skudai, Johor Bahru, Malaysia

²Department of Environmental Engineering, Curtin University, Malaysia, CDT 250, Miri 98009, Sarawak, Malaysia

³Department of Chemical Engineering, Lhokseumawe State Polytechnic, Lhokseumawe, Indonesia

⁴Department of Botany and Microbiology, College of Science, King Saud University, Riyadh, Saudi Arabia

*corresponding author e-mail address: hadibarata@curtin.edu.my | [16233109100](https://doi.org/10.33263/BRIAC95.394400)

ABSTRACT

Dyes wastewater is listed as one of the largest water polluter in this world and cause problems to the environment as well as human health. The present study aims to investigate the adsorption of methylene blue, a cationic dye commonly used in industries by activated carbon derived from the water hyacinth stem (*Eichhornia crassipes* (Mart.) Solms). The removal of MB solution was affected by some parameters such as dosage, contact time, pH, and initial dye concentration. The present study showed that the optimum condition for the adsorption process was pH 7, the adsorbent dosage at 0.8 g with the equilibrium was reached at 100 minutes. However, there is no significant adsorption in the effect of pH. It was found that the best correlation of kinetic with the MB adsorption was the pseudo-second-order model, while the isotherm study was well represented with the Freundlich model. The porosity of adsorbent was enhanced after carbonization process. The functional group presence on the surface of adsorbent including alcohols, carboxyl and carbonyl were also contributed to the effectiveness of adsorption process.

Keywords: Activated carbon; water hyacinth; methylene blue; textile wastewater; adsorption.

1. INTRODUCTION

In this era of industrialization, industrial wastewater has caused environmental pollution especially water pollution. Dyes and pigments can lead to water pollution and considered as one of the most serious environmental pollutant. Various manufactures such as cosmetic, cloth, and paper, consume dyes in their processes to color their final product. Textiles industries are listed as the first rank in the use of dye [1-2]. Annually, more than 106 tons' commercial dyes were produced by the industries and over 15% are disposed into wastewater and becoming contaminants to the environment. Dyes wastewater is harmful to aquatic life as well as human due to its carcinogenicity and toxicity. The presence of dye at low concentration in water bodies is highly visible and undesirable; hence reduce the aesthetic value [3]. Methylene blue is used widely in many industries to colorize their product such as cotton, paper, food, cosmetics, leather, etc. Methylene blue is not strongly hazard; it can cause difficulty in breathing, diarrhea, nausea, vomiting, confusion of mental and eye injury [4-5].

There are various methods to remove dyes from wastewater. The conventional wastewater treatment includes biological, chemical and physical treatment processes. Various conventional treatment was proposed to eliminate dyes from environment such as filtration, sedimentation, aerobic and anaerobic techniques, oxidation, and other physical and chemical process [6-13]. Although, those conventional methods showed their ability for eliminating dye at small scale, it can't be implemented in big scale or industrial scale due to high cost and energy utilization, generate a huge amount of by-product, and not ecofriendly. Therefore, efficiency is not sole factor in the selection of appropriate method,

but environmental and economical aspect needs to be considered such as requirement of raw materials and processing costs. Adsorption could be proposed as an alternative techniques for eliminating organic pollutant including because of low cost, operation simplicity, high selectivity and efficiency, and wide range implementation in various conditions [14-15]. Adsorption processes are reported as an effective and efficient method to decolorize wastewater. It involves the transfer of dye particles on adsorbent, thus resulting in clearer effluent. Carbon activation is a treatment that widely implemented because providing high porosity and effectiveness in the removal of dye. However, due to regeneration problem and expensive cost of activated carbon, researcher has found an alternative adsorbent [2, 16].

Water hyacinth (*Eichhornia crassipes* (Mart.); WH) is an aquatic plant originated from Latin America and widely spread all over the world. Currently, WH has become serious problems for many aquatic ecosystems such as the irrigation blockage, coverage of waterways, and place for mosquito breeding. WH is known for its extremely fast growing due to its abilities to remove pollutants from water and now considered as an important problem to aquatic biodiversity. It has exhibited extremely high densities in surface water and showed a damaging impact on the aquatic ecosystem and human population [17-18]. In this study the WH stem activated carbon was utilized for its ability to eliminate methylene blue (MB) from aqueous solution. The effect of some parameters such as dosage, contact time, pH, and initial dye concentration and the isotherm and kinetic study as well as the physical and chemical characterization of activated carbon was also analyzed and characterized.

2. MATERIALS AND METHODS

2.1. Adsorbent and dye preparation.

The water hyacinth (WH) was collected from water ecosystem in Puchong, Malaysia. WH was cleaned several times with tap water to remove dirt, then the stem is separated from the shoots and roots. The separated stem was cut into small pieces and dried in the oven at 110°C for 24 h. WH stem was impregnated with 10% ZnCl₂ solution and carbonized in a nitrogen-furnace (temperature 300°C) for 1 h. The pH of activated carbon was adjusted to pH7, and ground into 50-mesh sieve and stored in a desiccator. MB and other solvents were obtained from QRec, Malaysia. The physical and chemical property of MB is presented in Table 1. Batch studies were performed in agitated 100 mL-Erlenmeyer flask (120

rpm) containing 20ppm of dye. The filtration was conducted by using 0.45-μm regenerated cellulose membrane filter. All experiment was conducted in triplicate.

2.2. Characterization of activated carbon.

The physical microscopic of the WH was determined by using the FESEM analysis (FESEM, JEOL 6335f-SEM, Japan). The sample surface was coated with gold using splutter coater prior to FESEM analysis to derive the image. The role of functional group plays an important role in the adsorption of MB by WH was investigated by using Fourier Transform Infrared spectrometry (FTIR) (Spectrum One, Perkin Elmer, USA). The spectrum was set in the frequency range of 4000 to 450 cm⁻¹.

Table 1. Basic Information of MB.

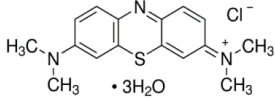
Aspect	Description
Name of Dye	Methylene Blue
Molecular Structure	
IUPAC Name	3,7-Bis(dimethylamino)phenothiazin-5-ium chloride
Empirical Formula	C ₁₆ H ₁₈ C ₁ N ₃ S · 3H ₂ O
Molecular Weight (g/mol)	373.90
Type of Dyes	Cationic (Basic)
Color	Blue or Dark green
Odor	Odorless
Dye composition	≥82 %
Solubility	H ₂ O: soluble (4mg/4ml)
Form	Powder

Table 2. Various experimental conditions on the adsorption of MB

	Parameters			
	pH	Dye concentration (ppm)	Adsorbent dosage (g)	Contact time (min)
Effect of pH	1-12	20	0.08	100
Effect of dye concentration	7	10-80	0.08	100
Effect of adsorbent dosage	7	20	0.01-0.1	100
Effect of contact time	7	20	0.08	1-180

2.3. Batch sorption studies.

The various experimental conditions are summarized in Table 2. The batch experiments were performed by adding various concentrations of MB in 100-ml conical flask. At the predetermined time, the flask was withdrawn from the shaker, filtered by using filter paper (125 mm) and the residual of the sample was measured using UV/Visible absorption spectrophotometry (CECIL CE7200 double-beam spectrophotometer) at wavelength 609 and 668nm. The experiment was performed in duplicate. The removal rate (%) and adsorption capacity (mg/g) were

$$\text{Removal rate (\%)} = \frac{C_0 - C_x}{C_0} \times 100 \quad (1)$$

$$\text{Adsorption Capacity (mg/g)} = A = \frac{(C_0 - C_x)V}{M} \quad (2)$$

Where A (mg/g) is the MB adsorption capacity, C₀ (mg/L) and C_x (mg/L) is initial and equilibrium of MB concentrations in the

solution, V (L) is the solution volume, and M (g) is the mass of adsorbent

2.4. Adsorption isotherm.

The adsorption isotherm study of the samples was conducted by manipulating the concentration of MB in experiments. Other parameters were controlled as optimized studied and were run for 24 h. To describe the best adsorption isotherms of MB onto the adsorbents, the following isotherm models were used:

$$\text{Langmuir equation: } \frac{C_e}{q_e} = \frac{1}{k_L q_m} + \frac{C_e}{q_m} \quad (3)$$

$$\text{Freundlich equation: } \ln q_e = \ln k_f + \left(\frac{1}{n}\right) \ln C_e \quad (4)$$

$$\text{Temkin equation: } q_e = B \ln A + B \ln C_e \quad (5)$$

Where C_e (mg/L) is the amount of MB at equilibrium, q_e (mg/g) is the amount of sorbed MB at equilibrium, q_m is the maximum sorption capacity, K_L is the Langmuir constant, K_F and n is the Freundlich constant, A is the Temkin equilibrium binding constant

(L/g) and B is the Temkin constant related to the heat of sorption (J mol^{-1}).

2.5. Adsorption kinetics.

The kinetic study of banana and coconut bunch adsorbent was carried for 38 h. Sample of solution was collected for the first 2 h and followed with a determining interval of time as shown in the table for further analysis. The initial concentration of MB was 20 ppm in 30ml of volume with an optimized parameter. The obtained data from the analytical method were then calculated for the removal rate (%) of MB and the adsorption capacity (mg/g).

3. RESULTS

3.1. Characterization of WH stem.

The FESEM images of raw WH stem, soaked WH stem, WH activated carbon and WH after treatment is presented in Fig. 1. The SEM images showed that the raw WHS has a smooth and plain surface. No pores were observed on the surface of raw WHS, whereas, a smaller pore was developed after being soaked with 1:1 of ZnCl_2 (soaked WH stem). After carbonization at 300 °C, a larger pore and the thicker the pore wall were developed on the surface of WH activated carbon. The surface of WH activated carbon was also rough compared to the surface of raw WH stem and soaked WH stem. Based on the images, the pores are occupied by MB molecules due to the formation of the white layer on the surface. The porosity and surface areas of WH activated carbon was enhanced by high temperature during carbonization process, together with, chemical activation by ZnCl_2 . This result was similar to previous studies that ZnCl_2 was acting as dehydrating agents and induced burning and prevents the tar formation. Addition of ZnCl_2 in activated carbon of adsorbents showed better surface morphology compared to without ZnCl_2 treatment. Smaller pore size and thicker pore walls were developed on the activated carbon treated with ZnCl_2 due to evaporation of chemical in the precursor during the carbonization process. The corrosive and dehydrating effect of ZnCl_2 has triggered the development of wider pores. Activated carbon of adsorbents treated with ZnCl_2 creates a larger surface area and pore volume compared to carbon treated with KOH and K_2CO_3 . A thicker porous wall and rough surface were observed on the surface of the carbon [19-20].

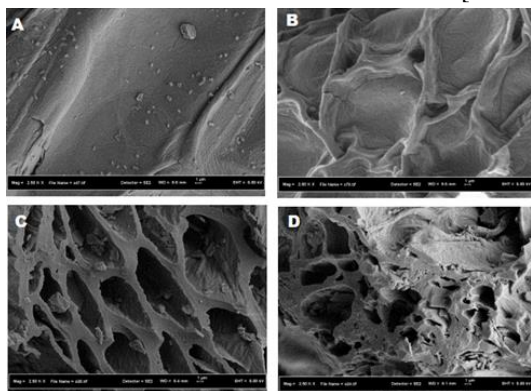


Figure 1. The FESEM images: raw WH stem (A), soaked with ZnCl_2 (B), activated carbon (C), and after treatment with MB solution (D).

The FTIR analysis of the WH was performed at range from 400 to 4000 cm^{-1} region (Fig. 2). Predominantly, a strong and broad peak appeared at 3409.72 cm^{-1} , 3407.87 cm^{-1} , 3426.86 cm^{-1} and

Then, to identify the best adsorption kinetic for the adsorbents, a kinetic model was used as follow:

$$\text{Pseudo-first-order model: } \ln(q_e - q_t) = \ln q_e - K_1 t \quad (6)$$

$$\text{Pseudo-second-order model: } \frac{t}{q_t} = \frac{1}{k_2 q_e^2} + \frac{t}{q_e} \quad (7)$$

Where q_e and q_t (mg/g) respectively indicate the amount 1 of the MB adsorbed at equilibrium and at time t (min); K_1 is the pseudo-first-order rate constant and K_2 is the pseudo-second order rate constant.

3393.90 cm^{-1} area due to the occurrence of alcohol and hydroxyl group ($-\text{OH}$). The hydroxyl group was also found at the region from 3200 to 3600 cm^{-1} on the surface of raw WH stem. However, WH activated carbon after adsorption, the stretching of $-\text{OH}$ group was weaker than stretching of $-\text{OH}$ vibration. A strong peak at 1627.92 cm^{-1} , 1626.47 cm^{-1} , 1615.53 cm^{-1} and 1613.08 cm^{-1} areas due to the existence of amines with $\text{N}-\text{O}$ stretch and at 1046.30 cm^{-1} and 1041.18 cm^{-1} shows that there was a group of alcohols, carboxylic acids, esters, or ethers. However, these peaks were weaker at spectra of WH activated carbon and WH after treatment. Probably, there was a reduction in groups of alcohols, carboxylic acids or esters during carbonization processes. Peak at 2923.63 cm^{-1} , 2923.87 cm^{-1} , and 2928.87 cm^{-1} was indicated as the presence of alkane with $\text{C}-\text{H}$ stretch. Small peaks were obtained 1409.38 cm^{-1} , 1400.16 cm^{-1} , 1387.27 cm^{-1} , and 1381.12 cm^{-1} that reducing of $\text{C}-\text{H}$ stretch WH activated carbon and WH after adsorption. Peak at 609.90 cm^{-1} , 600.64 cm^{-1} , 520.16 cm^{-1} and 527.39 cm^{-1} , there are assigned as the functional group of alkyl halides with $\text{C}-\text{Cl}$ stretch. The functional group presented on WH activated carbon such alcohols, carboxylic acids, and esters help the absorption of MB particles onto adsorbents (Table 3). These results were similar with previous studies that WH consists of natural cellulose like cotton, lignin and wax. The primary functional group of natural cellulose is hydroxyl group ($-\text{OH}$) that important for the sorption of MB. The hydroxyl group is active group that bond cationic dyes such as MB and positive charges of the adsorbates [21-22].

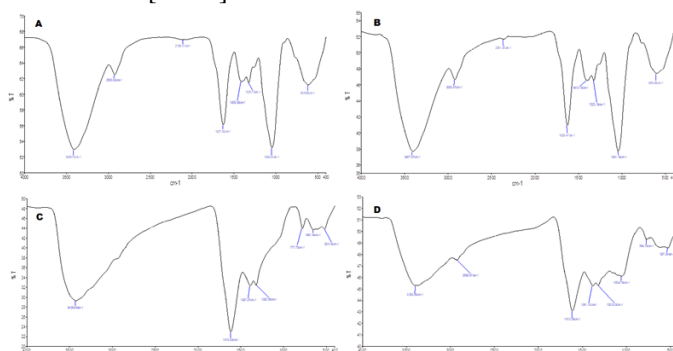


Figure 2. FTIR analyses: raw WH stem (A), soaked with ZnCl_2 (B), activated carbon (C), and after treatment with MB solution (D).

3.2. Batch studies.

The effect of some parameters on the removal of MB is shown in Table 3. Generally, there is no significant change in dye removal (91% to 97%) by varying the pH from 1 to 12. pH 7 showed the

maximum adsorption capacity (19.77 mg/g) and removal (97%), followed by pH 10 (96%) pH 3 (95%), pH 12 (94%), and pH 1 (91%). Principally, the interface between adsorbate and the active site is influenced by the surface charges on them. As the pH of the solution increased, the quantity of negative charged increased. Consequently, the negative charged will attract to the positive charge, hence improve the absorption of the dye. Low sorption of MB at lower pH is caused by the high quantity of hydrogen ion which effects in resistance of adsorption. The decrease of repulsion between the positively charged dye molecule and the adsorbent occurred at the high pH [23-25].

The MB removal was reduced from 99% to 67 % as the initial concentration increased from 10 ppm to 80 ppm. The percentage removal starts to decrease when the concentration was increased from 20 mg/L to 40 mg/L with a removal percentage 97% to 78%. This percentage removal versus initial concentration trend was similar to the study conducted by previous study. In contrast with the adsorption capacity, the capacity was increased when increasing the initial concentration. The adsorption capacity increased from 17.42 mg/g to 23.31 mg/g. The increasing in adsorption capacity when the initial concentration increase was due to the initial concentration that provides driving force to overcome all mass transfer resistance of the adsorbate between the aqueous and solid phase [26]. Therefore, a higher concentration of adsorbate would offer higher driving force and resulted high adsorption capacity. Another report showed that the ratio of active site to adsorbate concentration decreased with the increase in dye concentration [27-28].

On the effect of adsorbent dosage showed that the removal of MB was increased from 57 % to 99 % as the dosage of WHS-activated carbon increased from 0.01 to 0.1 g. The maximum removal recorded was at a dose of 0.1 g (99%). However, the adsorption

capacity was gradually increased from 10.74 mg/g to 19.07 mg/g for mass 0.01 g to 0.10 g. This experiment showed that the removal efficiency was dependent on the amount of adsorbent. Adsorbent dosage is the main factor that influences the uptake of dye onto adsorbent. The number of adsorbent dosage has strongly affected the removal of dyes It affects the capacity of adsorbent during adsorption take place [2, 26]. Previous studies showed that an increase in adsorbent dosage gave a continuous elimination which may be attributed to the saturation of binding sites due to aggregation of adsorbate [29-30]

The removal of MB was improved from 55 % to 99 % as the contact time increased from 1 min to 180 min while the highest adsorption capacity was 17.33 mg/g. MB was rapidly adsorbed in the first 4 min (55-82) and attains equilibrium in 100 min. No changes of removal were detected after equilibrium perceived, due to the presence of binding pore on adsorbent surface. Abundant of active pore on the surface of WH activated carbon in the first 4 minutes causes rapid adsorption and less number of accessible active site when equilibrium was reached. Similar trends were reported that the adsorption was gradually increased as the contact time increased and stagnant when equilibrium was reached. Previous study also showed the same result that rapid removal of MB by adsorbents was occurred in the first 20-25 min and reached equilibrium at 120 min. Surface adsorbent was gradually occupied at the initial stage of adsorption, causing low MB uptake after attaining equilibrium (Sachin and Gaikward [31]. The equilibrium time was depended on mass transfer rate or the situations for the interaction between the liquid and the solid stage. The removal was gradually decreased after 40 min due to the reduction in active site and binding pore availability [32-33]. The adsorption capacity of various adsorbents derived from agricultural biomass was given in Table 4.

Table 3. Effect some parameters on removal of MB by water hyacinth.

Treatment	Removal (%)	Adsorption capacity (mg/g)
Effect of pH		
pH1	90.61 ± 2.63	16.77 ± 0.07
pH3	94.98 ± 0.77	17.01 ± 0.15
pH7	97.29 ± 1.90	18.31 ± 0.38
pH10	95.91 ± 1.53	18.12 ± 0.49
pH12	93.89 ± 0.49	18.08 ± 1.00
Effect of dye concentration		
10 ppm	99.72 ± 1.56	17.42 ± 0.53
15 ppm	99.67 ± 0.00	17.99 ± 0.66
20 ppm	97.29 ± 1.90	18.31 ± 0.38
40 ppm	78.42 ± 0.42	20.72 ± 0.07
80 ppm	67.29 ± 1.90	23.31 ± 0.38
Effect of adsorbent dosage		
0.01 g	57.02 ± 0.97	10.74 ± 0.19
0.03 g	71.53 ± 0.34	13.56 ± 0.07
0.05 g	95.71 ± 0.12	18.05 ± 0.02
0.08 g	97.29 ± 1.90	18.31 ± 0.38
0.10 g	98.86 ± 0.05	19.07 ± 0.01
Effect of contact time		
1 min	55.12 ± 0.86	10.36 ± 0.18
4 min	82.54 ± 0.50	14.22 ± 0.16
10 min	86.02 ± 0.30	16.25 ± 0.08
50 min	95.77 ± 0.04	17.06 ± 0.01
100 min	97.29 ± 1.90	18.31 ± 0.38
120 min	98.83 ± 0.87	18.32 ± 0.17
180 min	98.89 ± 0.65	18.33 ± 0.13

Values are means of three experiments

Table 4. Adsorption capacities for activated carbons derived from agricultural wastes.

Adsorbents	Adsorption capacity (mg/g)	References
Corncob based activated carbon	0.8	[34]

Adsorbents	Adsorption capacity (mg/g)	References
Fir wood based activated carbon	1.2	[35]
Apricot stones-activated carbon	4.1	[36]
Coir pith carbon	5.8	[37]
Activated date pits	12.9	[38]
Activated olive stones	16.1	[38]
Water hyacinth activated carbon	18.3	This study

3.3. Isotherm and Kinetic Study.

The three most frequently used isotherm equations: Langmuir, Freundlich and Temkin equations were tested for the equilibrium data obtained from initial dye concentration study (Table 5). The models are simple, well-established and have physical meaning and are easily interpretable, which are some of the important reasons for their frequent and extensive use. The Langmuir isotherm model considers monolayer biosorption whereas Freundlich isotherm model describes biosorption onto a heterogeneous surface [39-40]. Temkin isotherm model is valid only for an intermediate range of ion concentrations and takes into account the effects of indirect adsorbate/adsorbate interactions on the adsorption process. This model also supposed that the heat of adsorption of all molecules in the layer decreases linearly as a result of increased surface coverage. The Langmuir constant, q_0 and K_L were determined by plotting a graph of $1/q_e$ against $1/C_e$. The value of q_0 and K_L were calculated from the intercept and slope respectively. Langmuir isotherm denotes to homogeneous monolayer adsorption. The Freundlich constant, K_F and n were obtained by plotting a graph of $\log q_e$ against $\log C_e$. The value of K_F and n were determined from the slope and intercept respectively. The Freundlich isotherm represents to the multilayer adsorption and for the adsorption on heterogeneous surfaces. It showed that the Langmuir and Temkin model was not fitted with experimental data due to low correlation coefficient value (R^2 ; 0.85 and 0.91). It was suggested that the isotherm study was fitted well into Freundlich models compared to other models. High correlation coefficient ($R^2=0.99$) revealed that the heterogeneity of the adsorption sites on WHS-activated carbon and multilayer of adsorption. The value of Freundlich exponent, $n=2.22$ was in the range of 1-10, indicate favorable adsorption. The big difference between amount of experimental, $q_{e\text{ exp}}$ (18 mg g^{-1}) and calculated adsorption capacity, $q_{e\text{ cal}}$ ($6.9 \times 10^{-49}\text{ mg g}^{-1}$) was obtained. If RL is larger than 1, the adsorption process is unfavorable, if it is equal to 1 it is linear and if it has a value between 0 and 1 it is favorable (occurs spontaneously) and if it is 0 it is irreversible [41]. The RL value calculated for reactive dyes for concentrations from 10 to 500 mg/L was found to be $0 < 1$. This situation shows the adsorption process occurs spontaneously.

Kinetics rate constant, k and q_e for each models can be calculated by plotting graph $\ln(q_e - q_i)$ versus t for pseudo-first-order, t/q_t versus t for pseudo-second-order models. Table 6 shows kinetic parameters obtained from calculated of the graph plotted. The amount of sorbed dyes (q_e) for each experiment is almost same as

4. CONCLUSIONS

The potential adsorbent derived from the WH stem AC were studied for MB removal in aqueous solution. Based on FESEM and FTIR analysis, it was observed that the effectiveness of the adsorption of MB onto WH stem was affected by surface

q_e calculated based on pseudo second order models. Furthermore, the R^2 obtained calculated through pseudo second order models for each experiments give value of 1.000 that prove it is better fit compare to pseudo-first-order. It suggested that the adsorption of MB followed the pseudo second order. It is obviously shown that a high correlation coefficient, ($R^2=0.999$) was obtained. Also, there is a small difference between the amount of experimental ($q_{e\text{ exp}} = 18.1\text{ mg/g}$) and the calculated adsorption capacity ($q_{e\text{ cal}} = 17.4\text{ mg/g}$). Thus, the data obtained suggested that the adsorption of MB onto WHS-activated carbon obeyed the pseudo-second-order kinetic. Previous study showed that the pseudo-second-order was better kinetic analysis for the adsorption of Dark Blue GL onto WH with correlation of $R^2 = 0.99$ [42]. The correlation coefficients (R^2) for the pseudo-second-order kinetic model are higher than the other kinetic models. The q_e values calculated from pseudo second order kinetic model are also close to the experimental data. Thus, pseudo-second-order kinetic is more appropriate to define the adsorption process. If a sufficient mixture is provided, the film diffusion rate increases toward the limiting rate factor of the pore diffusion point [43-44]. The result showed that the pseudo-first-order kinetic is not best to describe the experimental data. This states that chemical sorption involving valence force induced by sharing or exchange of electrons between adsorbate and adsorbent is the rate controlling step [45-46].

Table 5. Isotherm parameters for adsorption of MB onto WH stem.

Adsorption isotherm	Adsorption constant	Value
Langmuir	q_m (mg/g)	0.29
	K_L (mg/L)	-0.265
	R^2	0.85
Freundlich	n	2.22
	K_L (mg/g)	1.58
	R^2	0.99
Temkin	A	19.37
	B	36.823
	R^2	0.91

Table 6. The kinetic parameter of adsorption of MB onto WH stem

Adsorption kinetic	Parameter	Value
Pseudo-first-order	$q_{e\text{ exp}}$ (mg/g)	18.09
	$q_{e\text{ cal}}$ (mg/g)	6.855×10^{-49}
	K_1	0.928
	R^2	18.090
Pseudo-second-order	$q_{e\text{ exp}}$ (mg/g)	17.425
	$q_{e\text{ cal}}$ (mg/g)	0.047
	K_1	0.999
	R^2	

functional group and surface morphology. The porosity of adsorbent was enhanced after carbonization process. The functional group presence on the surface of adsorbent including alcohols, carboxyl and carbonyl were also contributed to the

effectiveness of adsorption process. The removal of MB solution was affected by contact time, initial dye concentration and adsorbent dosage. This present study showed that the optimum condition for the adsorption process was pH 7, the adsorbent dosage at 0.8 g with the equilibrium was reached at 100 minutes.

5. REFERENCES

- Adnan, L.A.; Mohd Yusoff, A.R.; Hadibarata, T.; Khudhair, A.B. Biodegradation of Bis-Azo Dye Reactive Black 5 by White-Rot Fungus *Trametes gibbosa* sp. WRF 3 and Its Metabolite Characterization. *Water Air Soil Pollut* **2014**, *225*, 2119, <https://doi.org/10.1007/s11270-014-2119-2>.
- Rahmat, N.A.; Ali, A.A.; Salmiati; H.N.; Muhamad, M.S.; Kristanti, R.A.; Hadibarata, T. Removal of Remazol Brilliant Blue R from Aqueous Solution by Adsorption Using Pineapple Leaf Powder and Lime Peel Powder. *Water Air Soil Pollut* **2016**, *227*, 105, <https://doi.org/10.1007/s11270-016-2807-1>.
- Ben, A.R.; Karoui, S.; Mougin, K.; Ghorbal, A. Adsorptive removal of cationic and anionic dyes from aqueous solution by utilizing almond shell as bioadsorbent. *Euro-Mediterr J Environ Integr* **2017**, *2*, 20, <https://doi.org/10.1007/s41207-017-0032-y>.
- Lazim, Z.M.; Mazuin, E.; Hadibarata, T.; Yusop, Z. The removal of methylene blue and Remazol Brilliant Blue R dyes by using orange peel and spent tea leaves. *J Teknologi* **2015**, *74*, 129-135, <https://doi.org/10.11113/jt.v74.4882>.
- Kristanti, R.A.; Kamisan, M.K.A.; Hadibarata, T. Treatability of Methylene Blue Solution by Adsorption Process Using *Neobalanocarpus hepmii* and *Capsicum annum*. *Water Air Soil Pollut* **2016**, *227*, 134, <https://doi.org/10.1007/s11270-016-2834-y>.
- Thung, W.; Ong, S.; Ho, L.; Wong, Y.; Fahmi, R.; Harvinder Kaur, L.; Oon, Y.; Oon, Y. Biodegradation of Acid Orange 7 in a combined anaerobic-aerobic up-flow membrane-less microbial fuel cell: mechanism of biodegradation and electron transfer. *Chem Eng J* **2018**, *336*, 397-405, <https://doi.org/10.1016/j.cej.2017.12.028>.
- Al Farraj, D.A.; Hadibarata, T.; Yuniarto, A.; Syafiuddin, A.; Surtikanti, H.K.; Elshikh, M.S.; Al Khulaifi, M.M.; Al-Kufaidy, R. Characterization of pyrene and chrysene degradation by halophilic *Hortaea* sp. B15. *Bioproc Biosyst Eng* **2019**, *42*, 963-969, <https://doi.org/10.1007/s00449-019-02096-8>.
- Lazim, Z. M.; Hadibarata, T. Ligninolytic fungus *Polyporus* sp. S133 mediated metabolic degradation of fluorene. *Brazilian J Microbiol* **2016**, *47*, 610-6, <https://doi.org/10.1016/j.bjm.2016.04.015>.
- Nor, N.M.; Hadibarata, T.; Zubir, M.M.; Lazim, Z.M.; Adnan, L.A.; Fulazzaky, M.A. Mechanism of triphenylmethane Cresol Red degradation by *Trichoderma harzianum* M06. *Bioproc Biosyst Eng* **2015**, *38*, 2167-75, <https://doi.org/10.1007/s00449-015-1456-x>.
- Bate, N.; Shi, H.; Chen, L.; Wang, J.; Xu, S.; Chen, W.; Li, J.; Wang, E. Micelle-Directing Synthesis of Ag-Doped WO₃ and MoO₃ Composites for Photocatalytic Water Oxidation and Organic-Dye Adsorption. *Chem Asian J* **2017**, *12*, 2597-2603, <https://doi.org/10.1002/asia.201700951>.
- Barbosa, A.A.; de Aquino, R.V.S.; da Cruz, N.S.; Dantas, R. F.; Duarte, M.; Rossiter Sa da Rocha, O. Kinetic study of dye removal using TiO₂ supported on polyethylene terephthalate by advanced oxidation processes through neural networks. *Water Sci Technol* **2019**, *79*, 1134-1143, <https://doi.org/10.2166/wst.2019.111>.
- Salazar, R.; Ureta-Zanartu, M.S.; Gonzalez-Vargas, C.; Brito, C.D.N.; Martinez-Huitile, C.A. Electrochemical degradation of industrial textile dye disperse yellow 3: Role of electrocatalytic material and experimental conditions on the catalytic production of oxidants and oxidation pathway. *Chemosphere* **2018**, *198*, 21-29, <https://doi.org/10.1016/j.chemosphere.2017.12.092>.
- Cui, M.H.; Sangeetha, T.; Gao, L.; Wang, A.J. Efficient azo dye wastewater treatment in a hybrid anaerobic reactor with a built-in integrated bioelectrochemical system and an aerobic biofilm reactor: Evaluation of the combined forms and reflux ratio. *Biores Technol* **2019**, *122001*, <https://doi.org/10.1016/j.biortech.2019.122001>.
- Adnan, L.A.; Sathishkumar, P.; Yusoff, A.R.; Hadibarata, T.; Ameen, F. Rapid bioremediation of Alizarin Red S and Quinizarine Green SS dyes using *Trichoderma lixii* F21 mediated by biosorption and enzymatic processes. *Bioproc Biosyst Eng* **2017**, *40*, 85-97, <https://doi.org/10.1007/s00449-016-1677-7>.
- Anastopoulos, I.; Margiotoudis, I.; Massas, I. The use of olive tree pruning waste compost to sequester methylene blue dye from aqueous solution. *Int. J. Phytoremediation* **2018**, *20*, 831-838, <https://doi.org/10.1080/15226514.2018.1438353>.
- Mostafa, A.A.; Elshikh, M.S.; Al-Askar, A.A.; Hadibarata, T.; Yuniarto, A.; Syafiuddin, A. Decolorization and biotransformation pathway of textile dye by *Cylindrocephalum aurelium*. *Bioproc Biosyst Eng* **2019**, *42*, 121-128, <https://doi.org/10.1007/s00449-019-02144-3>.
- Sindhu, R.; Binod, P.; Pandey, A.; Madhavan, A.; Alphonsa, J. A.; Vivek, N.; Gnansounou, E.; Castro, E.; Faraco, V. Water hyacinth a potential source for value addition: An overview. *Bioresour. Technol.* **2017**, *230*, 152-162, <https://doi.org/10.1016/j.biortech.2017.01.035>.
- Bulgariu, L.; Escudero, L.B.; Bello, O.S.; Iqbal, M.; Nisar, J.; Adegoke, K.A.; Alakhras, F.; Kornaros, M.; Anastopoulos, I. The utilization of leaf-based adsorbents for dyes removal: A review. *J. Mol. Liq.* **2019**, *276*, 728-747, <https://doi.org/10.1016/j.molliq.2018.12.001>.
- Wirasmita, R.; Hadibarata, T.; Yusoff, A.R.M.; Yusop, Z. Removal of Bisphenol A from Aqueous Solution by Activated Carbon Derived from Oil Palm Empty Fruit Bunch. *Water Air Soil Pollut* **2014**, *225*, 2148, <https://doi.org/10.1007/s11270-014-2148-x>.
- Saratale, R.G.; Sivapathan, S.S.; Jung, W.J.; Kim, H.Y.; Saratale, G.D.; Kim, D.S. Preparation of activated carbons from peach stone by H₄P₂O₇ activation and its application for the removal of Acid Red 18 and dye containing wastewater. *J Environ Sci Health A Tox Hazard Subst Environ Eng* **2016**, *51*, 164-177, <https://doi.org/10.1080/10934529.2015.1087747>.
- Noeline, B.F.; Manohar, D.M.; Anirudhan, T.S. Kinetic and equilibrium modelling of lead(II) sorption from water and wastewater by polymerized banana stem in a batch reactor. *Sep. Purif. Technol.* **2005**, *45*, 131-140, <https://doi.org/10.1016/j.seppur.2005.03.004>.
- Hameed, B.H.; Hakimi, H. Utilization of durian (*Durio zibethinus* Murray) peel as low cost sorbent for the removal of acid dye from aqueous solutions. *Biochem. Eng. J.* **2008**, *39*, 338-343, <https://doi.org/10.1016/j.bej.2007.10.005>.
- Saeed, A.; Sharif, M.; Iqbal, M. Application potential of grapefruit peel as dye sorbent: kinetics, equilibrium and

- mechanism of crystal violet adsorption. *J Hazard Mater* **2010**, *179*, 564-72, <https://doi.org/10.1016/j.jhazmat.2010.03.041>.
24. Ahmad, R. Studies on adsorption of crystal violet dye from aqueous solution onto coniferous pinus bark powder (CPBP). *J Hazard Mater* **2009**, *171*, 767-73, <https://doi.org/10.1016/j.jhazmat.2009.06.060>.
25. Sanmuga, P.E.; Senthamil, S.P. Water hyacinth (Eichhornia crassipes) – An efficient and economic adsorbent for textile effluent treatment – A review. *Arabian J Chem* **2017**, *10*, S3548-S3558, <https://doi.org/10.1016/j.arabjc.2014.03.002>.
26. Lazim, Z.M.; Hadibarata, T.; Puteh, M.H.; Yusop, Z. Adsorption Characteristics of Bisphenol A onto Low-Cost Modified Phyto-Waste Material in Aqueous Solution. *Water Air Soil Pollut* **2015**, *226*, 34, <https://doi.org/10.1007/s11270-015-2318-5>.
27. Ahmad, R.; Kumar, R. Adsorption studies of hazardous malachite green onto treated ginger waste. *J. Environ. Manage.* **2010**, *91*, 1032-1038, <https://doi.org/10.1016/j.jenvman.2009.12.016>.
28. Lin, Y.; He, X.; Han, G.; Tian, Q.; Hu, W. Removal of crystal violet from aqueous solution using powdered mycelial biomass of *Ceriporia lacerata* P2. *J Environ Sci (China)* **2011**, *23*, 2055-62, [https://doi.org/10.1016/S1001-0742\(10\)60643-2](https://doi.org/10.1016/S1001-0742(10)60643-2).
29. Muthukumar, C.; Sivakumar, V.M.; Thirumarimurugan, M. Adsorption isotherms and kinetic studies of crystal violet dye removal from aqueous solution using surfactant modified magnetic nanoadsorbent. *J Taiwan Inst Chem Eng* **2016**, *63*, 354-362, <https://doi.org/10.1016/j.jtice.2016.03.034>.
30. Silveira, M.B.; Pavan, F.A.; Gelos, N.F.; Lima, E.C.; Dias, S.L.P. Punica granatum Shell Preparation, Characterization, and Use for Crystal Violet Removal from Aqueous Solution. *CLEAN – Soil Air Water* **2014**, *42*, 939-946, <https://doi.org/10.1002/clean.201100722>.
31. Sachin, M.K.; Gaikward, R.W. Removal of Methylene Blue from Effluent by Using Activated Carbon and Water Hyacinth as Adsorbent. *Int J Chem EngAppl* **2011**, *2*, 319, <https://doi.org/10.7763/IJCEA.2011.V2.126>.
32. Ratnamala, G.M.; Shetty, K.V.; Srinikethan, G. Removal of Remazol Brilliant Blue Dye from Dye-Contaminated Water by Adsorption Using Red Mud: Equilibrium, Kinetic, and Thermodynamic Studies. *Water Air Soil Pollut* **2012**, *223*, 6187-6199, <https://doi.org/10.1007/s11270-012-1349-4>.
33. Volesky, B. Detoxification of metal-bearing effluents: biosorption for the next century. *Hydrometallurgy* **2001**, *59*, 203-216, [https://doi.org/10.1016/S0304-386X\(00\)00160-2](https://doi.org/10.1016/S0304-386X(00)00160-2).
34. Tseng, R.L.; Tseng, S.K.; Wu, F.C. Preparation of high surface area carbons from Corn cob with KOH etching plus CO₂ gasification for the adsorption of dyes and phenols from water. *Colloids Surf. Physicochem. Eng. Aspects* **2006**, *279*, 69-78, <https://doi.org/10.1016/j.colsurfa.2005.12.042>.
35. Wu, F.C.; Tseng, R.L. High adsorption capacity NaOH-activated carbon for dye removal from aqueous solution. *J. Hazard. Mater.* **2008**, *152*, 1256-1267, <https://doi.org/10.1016/j.jhazmat.2007.07.109>.
36. Aygün, A.; Yenisooy-Karakaş, S.; Duman, I. Production of granular activated carbon from fruit stones and nutshells and evaluation of their physical, chemical and adsorption properties. *Microporous Mesoporous Mater.* **2003**, *66*, 189-195, <https://doi.org/10.1016/j.micromeso.2003.08.028>.
37. Kavitha, D.; Namasivayam, C. Experimental and kinetic studies on methylene blue adsorption by coir pith carbon. *Bioresour. Technol.* **2007**, *98*, 14-21, <https://doi.org/10.1016/j.biortech.2005.12.008>.
38. Alaya, M.N.; Hourieh, M.A.; Youssef, A.M.; El-Sejarah, F. Adsorption Properties of Activated Carbons Prepared from Olive Stones by Chemical and Physical Activation. *Adsorpt Sci Technol* **2000**, *18*, 27-42, <https://doi.org/10.1260/0263617001493251>.
39. Langmuir, I. The adsorption of gases on plane surfaces of glass, mica and platinum. *J. Am. Chem. Soc.* **1918**, *40*, 1361-1403, <https://doi.org/10.1021/ja02242a004>.
40. Freundlich, H. Über die Adsorption in Lösungen. In *Z. Phys. Chem.*, 1907; Volume 57U, pp. 385, <https://doi.org/10.1515/zpch-1907-5723>.
41. Ooi, J.; Lee, L.Y.; Hiew, B.Y.Z.; Thangalazhy-Gopakumar, S.; Lim, S.S.; Gan, S. Assessment of fish scales waste as a low cost and eco-friendly adsorbent for removal of an azo dye: Equilibrium, kinetic and thermodynamic studies. *Bioresour Technol* **2017**, *245*, 656-664, <https://doi.org/10.1016/j.biortech.2017.08.153>.
42. Khan, M.M.R.; Mukhlis, M.Z.B.; Mazumder, M.S.I.; Ferdous, K.; Prasad, D.M.R.; Hassan, Z. Uptake of Indosol Dark-blue GL dye from aqueous solution by water hyacinth roots powder: adsorption and desorption study. *Int J Environ Sci Technol* **2014**, *11*, 1027-1034, <https://doi.org/10.1007/s13762-013-0363-4>.
43. Ge, H.; Wang, C.; Liu, S.; Huang, Z. Synthesis of citric acid functionalized magnetic graphene oxide coated corn straw for methylene blue adsorption. *Bioresour Technol* **2016**, *221*, 419-429, <https://doi.org/10.1016/j.biortech.2016.09.060>.
44. Zhang, Y.; Wang, W.; Zhang, J.; Liu, P.; Wang, A. A comparative study about adsorption of natural palygorskite for methylene blue. *Chem Eng J* **2015**, *262*, 390-398, <https://doi.org/10.1016/j.cej.2014.10.009>.
45. Ho, Y.S.; McKay, G. Pseudo-second order model for sorption processes. *Process Biochemistry* **1999**, *34*, 451-465, [https://doi.org/10.1016/S0032-9592\(98\)00112-5](https://doi.org/10.1016/S0032-9592(98)00112-5).
46. Ho, Y.S. Review of second-order models for adsorption systems. *J. Hazard. Mater.* **2006**, *136*, 681-689, <https://doi.org/10.1016/j.jhazmat.2005.12.043>.

6. ACKNOWLEDGEMENTS

This research was supported by AUN/Seed Net, Collaborative Research Program for Common Regional Issues (CRC), JICA No. 4B231



© 2019 by the authors. This article is an open access article distributed under the terms and conditions of the Creative Commons Attribution (CC BY) license (<http://creativecommons.org/licenses/by/4.0/>).